Publishing House
AKAPIT

COMPUTER METHODS IN MATERIALS SCIENCE

Informatyka w Technologii Materiałów

Vol. 10, 2010, No. 4

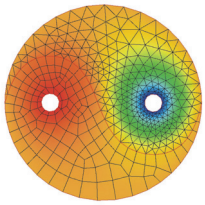

NUMERICAL PREDICTION OF MICROSTRUCTURE IN HIGH-STRENGTH DUCTILE FORGING PARTS

ARTHUR BACK[1]*, MARCUS URBAN[1], CHRISTOPH KEUL[2], WOLFGANG BLECK[2], GERHARD HIRT[1]

[1] *Institute of Metal Forming (IBF), RWTH Aachen University, Aachen, Germany*
[2] *Institute of Ferrous Metallurgy (IEHK), RWTH Aachen University, Aachen, Germany*
**Corresponding author: back@ibf.rwth-aachen.de*

Abstract

The automotive industry has an ongoing request for lighter, stiffer and at the same time cheaper parts to maintain the economic and technical progress. Especially in case of safety relevant components a combination of high stiffness and sufficient ductility is required. Regarding these demands the main subject of this project was to improve the mechanical properties of forging steel alloys by employing a high-strength and ductile bainitic microstructure while maintaining a cost effective process chain for the high-stressed forged parts. For these purposes a new steel alloy with an optimized process chain has been developed. To reduce the experimental effort for identifying the process parameters and geometries that enable the target microstructure a numerical approach was developed to predict the microstructure of the steel alloy after the process chain. The implemented numerical approach is based on FEM simulations of the forging and cooling combined with deformation-cooling-time-temperature-transformation diagrams.

Key words: FEM, forging, cooling, microstructure prediction, steel alloy development

1. INTRODUCTION

The automotive industry has a steady request for weight reduced components combined with high mechanical properties. Generally ferritic-perlitic precipitation hardening steels or quenched and tempered (Q&T) steels are used in forging processes for light, stiff and cost efficient products. The benefits of these ferritic-perlitic precipitation steels towards Q&T steels are avoiding a heat treatment step, improved machinability and more homogenous properties (Cristinacce & Reynolds, 1996; Gladman, 1997). But these steels do not exhibit sufficient toughness values and are limited in their level of strength as compared with the Q&T steels. Hence, new alloying concepts and optimized forging parameters have to be identified to enable high strength and sufficient ductility at room temperature without additional quenching. A promising way to reach these goals with minimum costs is to guarantee bainitic microstructures in the forged parts after continuous cooling at resting air (Bhadeshia, 2001; Lemaitre & Dierickx, 2006). The high ductile bainitic (HDB) steel developed within this project enables an ultimate tensile strength (R_m) of the material combined with a high elongation at fracture (A_5) and an impact toughness (Av) at room temperature that reaches or exceeds the target values as shown in table 1.

Table 1. *Target mechanical properties.*

$R_{p0,2}$	R_m	Av	A_5
850 MPa	1200 MPa	27 J	10%

The need of a bainitic microstructure in the part after forging and cooling at resting air calls

 ISSN 1641-8581

for a defined cooling strategy depending on the temperature and plastic strain after forging. As a result there is a high experimental effort for optimizing the process parameters and identifying geometries that enable the bainitic microstructure in the part after forging and cooling at resting air for the specified steel. To reduce the experimental expense a simulation module has been developed to predict the microstructure and hardness in the forged part after the process chain.

2. ALLOYING CONCEPT

The main objective within this project was to develop a steel alloy which offers high strength as well as a sufficient ductility. As documented in literature, a bainitic microstructure is a promising way to obtain these properties (Bhadeshia, 2001). For further optimization the alloying concept of 25MnCrSiVB6 was chosen as the reference material. This alloy has shown the possibility to reach bainitic microstructure with tensile strength up to 1030 MPa (Lemaitre & Dierickx, 2006). Based on this steel, the alloying concept was altered in order to get a slowly transforming alloy, which provides a broad bainitic phase field and retards the purely diffusion controlled ferrite/pearlite phase transformations. In dilatometer tests an alloying concept with the chemical composition as shown in table 2 has been found adequate to enlarge the bainitic area in the (deformation)-cooling-time-transformation diagram ((D)CTT-diagram) and therefore reaches satisfying mechanical values at room temperature. The two steels Pilot 1 and Pilot 2 differ in their carbon content.

***Table 2**. Chemical composition of HDB steel alloys in weight %.*

	C	Si	Mn	P	S	Cr	Mo	Al	Nb	Ti	N
Pilot 1	0,18	1,53	1,47	0,01	0,01	1,30	0,07	0,02	0,03	0,025	0,008
Pilot 2	0,22	1,47	1,50	0,01	0,01	1,31	0,09	0,02	0,03	0,025	0,011

The (D)CTT diagram, such as shown in figure 1, is an alternative to the conventional continuous-cooling-transformation diagram (CCT diagram) to display the share of the microstructure and hardness after the cooling of the material depending on the plastic strain, forming temperature and exponential cooling rate (Newtons' cooling) (Fang et al., 2009). The main difference between both types of diagrams concerns the temporal representation. Here the characteristic of the CTT diagram is to present the phases and the hardness that occur after continuous cooling of the material depending on the time $t_{8/5}$ that the material needs to cool down from 800°C to 500°C. Furthermore, the (D)CTT diagram can be arranged in tables and evaluated by numeric routines.

2.1. Microstructure

To provide (D)CTT diagrams for different plastic strains and forming temperatures a quantitative description of the phase fractions in the microstructure is required. The necessary data can be obtained on the basis of light optical metallography (LOM) and scanning electron microscopy (SEM). The detailed description of the bainitic microstructure is done by an object based image analysis of SEM micrographs (Fischer et al., 2009). This method is based on the automatic detection of structures on different scale levels and allows classifying the microstructure with respect to the shape of objects, spatial distribution and the relationship between objects. Figure 1 shows a representative for a (D)CTT diagram presenting the transformation properties of the new developed HDB-steel Pilot 2. Herein information for a state with no plastic strain is provided as well as for a state with an applied strain (ε) of 1.0 at two different forming temperatures (T_f = 1000, 1100°C).

2.2. Material Properties

When modeling the forging and cooling processes in the FEM-simulation a detailed description of the material properties is required. The HDB-steel has a density of 7850 kg/m³ and a Young's Modulus of 210 GPa. The results for the conductivity gained by using the Laser-Flash Method and the results for the specific heat capacity measured by Differential Scanning Calorimetry (DSC) are shown in figure 2 and figure 3, respectively. For simulating the forging process the flow curve was determined in compression tests for temperatures between 950°C and 1250°C and strain rates between 0.001 s^{-1} and 1 s^{-1}.

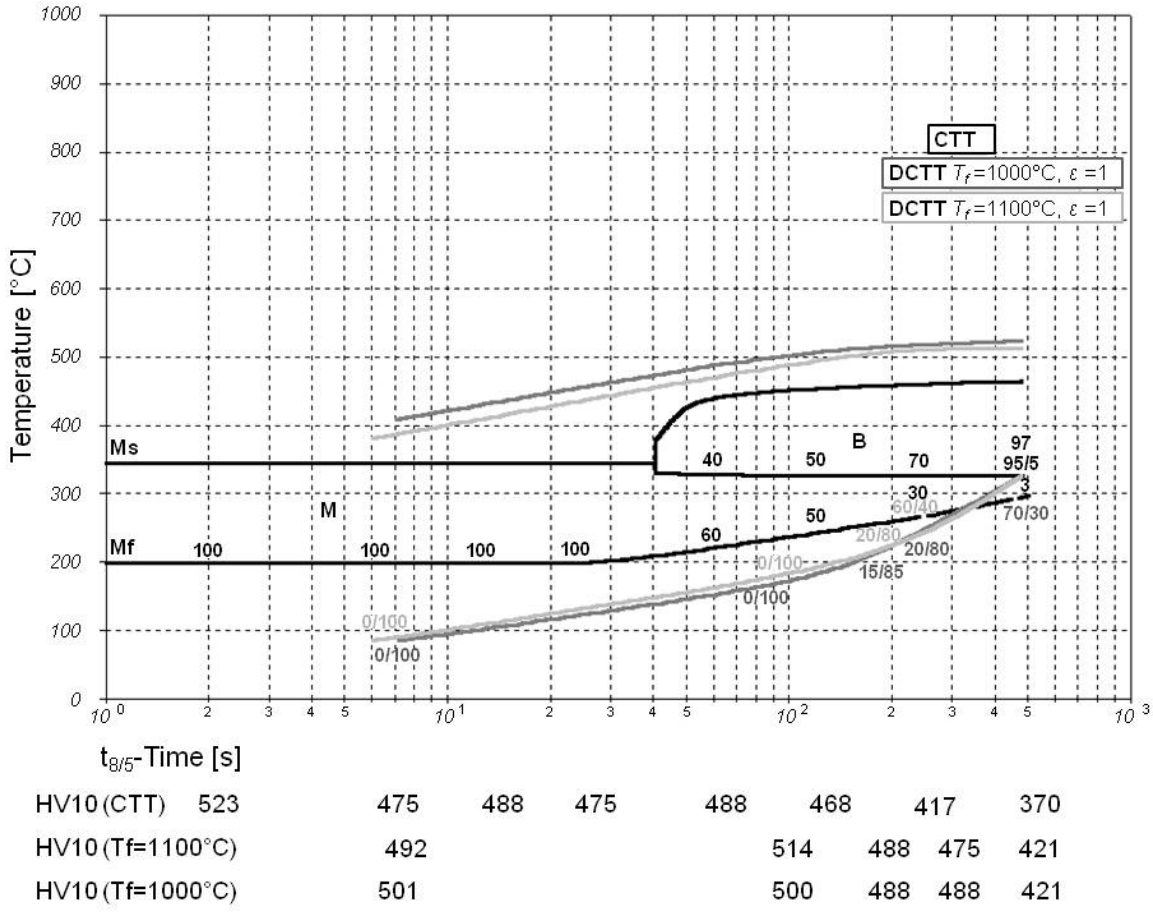

Fig. 1. *(D)CTT of the new HDB-steel Pilot 2.*

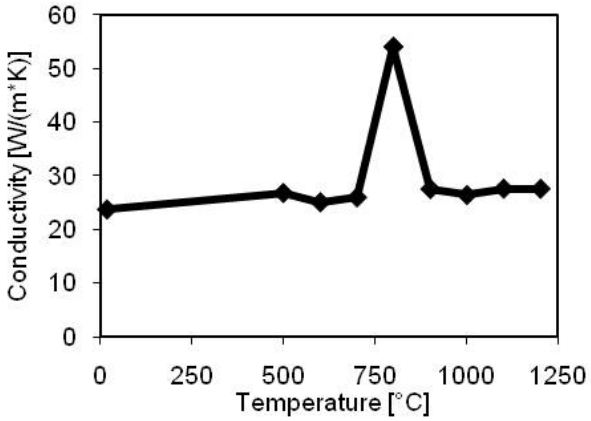

Fig. 2. *Conductivity of the HDB-steel.*

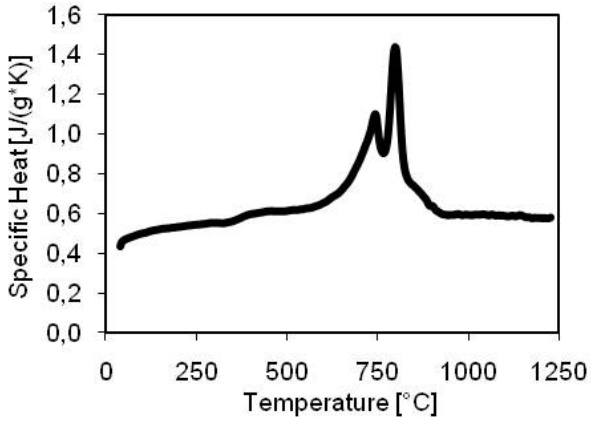

Fig. 3. *Specific heat of the HDB-steel.*

In order to identify the radiation of the HDB-steel cooling tests were combined with FEM-simulations using the implicit Larstran/Shape solver. With the aforementioned results for density, specific heat capacity and heat conductivity the only unknown variables for the FEM-simulation using Larstran/Shape are the heat emissivity (ε) at resting air and the heat transfer coefficient (α) between HDB-steel and air. To identify these values in an experiment, cylindrical specimens with a diameter of 20 mm and a height of 20 mm were heated up to 1250°C and subsequently cooled at resting air. The simulated temperature-time history resulting from the cooling process is compared to the data measured with thermocouples in the experiment. Finally, the best agreement between the simulated and experimental measured temperature-time results was achieved with a heat transfer coefficient of 5.6E-05 W/(mm²K) and a heat emissivity of 0.96 (figure 4).

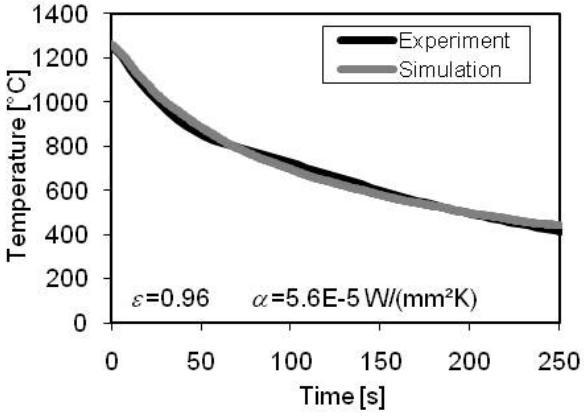

Fig. 4. Temperature time history in the middle of a cylindrical specimen during cooling.

3. NUMERICAL PREDICTION OF MICROSTRUCTURE

The implemented numerical approach utilizes the results of the FEM-simulations of the forging and cooling process in order to correlate them with the data contained in the (D)CTT diagrams. An overview on the single steps of the prediction method is given in figure 5.

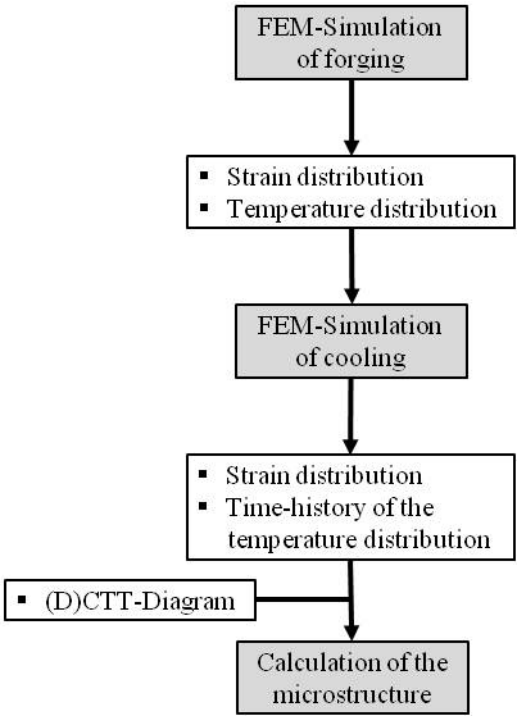

Fig. 5. Process of microstructure prediction.

In a first step the user has to run a FEM-simulation for the forging process to receive the forged geometry with its mechanical properties. Main results for the further use are the strain and temperature distributions after the forging process in the part. In the next step, the cooling at resting air is simulated in order to get the time history of the temperature distribution. With the temperature-time history the $t_{8/5}$-time can be calculated for each node of the FEM-mesh. Due to the stepwise strategy of the FE-method the simulation time has to be interpolated in order to identify the time when the node has a temperature of 800°C and 500°C, respectively (see figure 6). The difference between these interpolated times is the $t_{8/5}$-time.

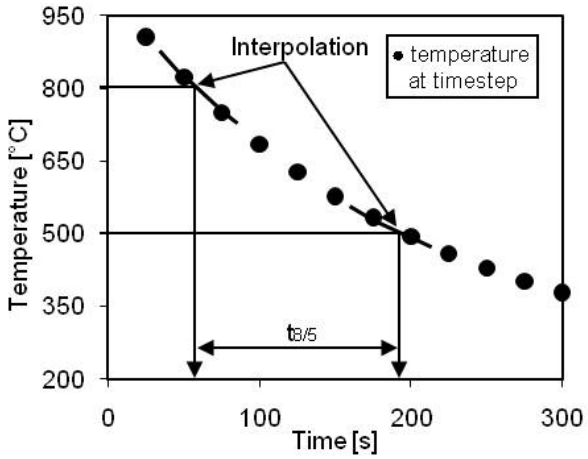

Fig. 6. Interpolation between exported timesteps.

The resulting microstructure and hardness are affected by the strain, the temperature after forging and the temperature-time history of the cooling process. In consequence (D)CTT diagrams for different plastic strains and temperatures after forging have to be recorded and supplied to the prediction method in the form of tables.

3.1. Extrapolation

When calculating the $t_{8/5}$-time the case that the temperature at an area of the component after forging may be close to or even below 800°C must be taken into account, see figure 7. Interpolating the temperature-time history to determine the time when this area has a temperature of 800°C in the continuous cooling of the part is not possible or leads to high $t_{8/5}$ values which do not represent the fractures of microstructure that occur in the experiment.

The formation of the bainite microstructure during the continuous cooling arises at temperatures between 450°C and 350°C (see figure 1). As a result the cooling rates at lower temperatures are of major importance. In comparison with experimental results better prediction of the microstructure was achieved when the extrapolation of the temperature-time history started at the point of inflection, as shown in figure 7. For the extrapolation the temperature-time

history is approximated by the equation (1), where T is the temperature and t is the time since the beginning of the cooling process. The constant parameters a, b and c have to be determined for each extrapolation.

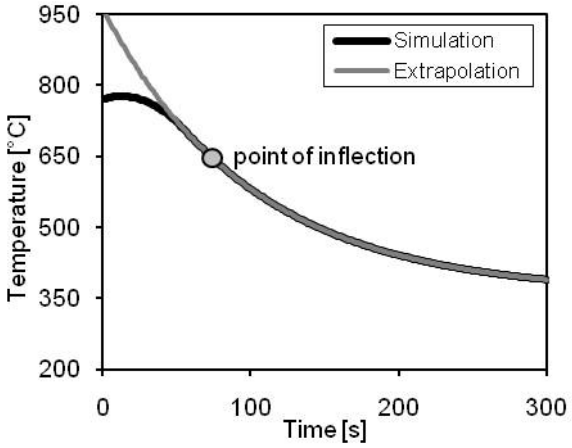

Fig. 7. *Extrapolation of the temperature-time history.*

$$T = a + b\mathrm{e}^{-c \cdot t} \tag{1}$$

The constant parameters can be identified by applying the least square method. Using the least square method implies to determine the unknown parameters so much that the sum of the square of the deviation between exported temperature T_i at the time t_i of the FEM-simulation of the cooling process and the calculated values of equation (1) at the time t_i reaches its minimum:

$$\min\{G\} = \min\{\Sigma_i[(a + b \cdot \mathrm{e}^{-c \cdot t_i}) - T_i]^2\} \tag{2}$$

This requirement is reached when the derivations of G with respect to the parameters a, b and c equals 0 (see equation (3)) and the second derivation is higher than 0.

$$\frac{\partial G}{\partial a} = \frac{\partial G}{\partial b} = \frac{\partial G}{\partial c} = 0 \tag{3}$$

However this system of equations cannot be solved directly due to the non-linearity of the function G. On the assumption that the parameter a is known, equation (2) can be linearized and the parameters b and c can be identified using equation (7).

$$\min\{\mathrm{F}\} = \min\{\Sigma_i[(z + c \cdot t_i) - d_i]^2\} \tag{4}$$

with

$$z = \ln(b) \tag{5}$$

$$d_i = \ln(T_i - a) \tag{6}$$

$$\frac{\partial F}{\partial z} = \frac{\partial F}{\partial c} = 0 \tag{7}$$

In order to identify the parameter a the hill-climbing optimization is used (Johnson & Jacobson, 2002). As the hill-climbing optimization identifies local optimum, the initial estimation of a is very important. To provide an initial estimation of a close to its optimal value, equation (1) is linearized by its derivation by time:

$$\ln(\dot{T}) = \ln(bc) + ct \tag{8}$$

Solving equation (9) allows identifying the parameters b and c.

$$\min\{H\} = \min\{\Sigma_i[\ln(bc) + ct - \ln(\dot{T}_i)]^2\} \tag{9}$$

A start value of a for the hill-climbing optimization can be calculated by inserting b and c in equation (2).

4. EXPERIMENTAL VALIDATION

To enable the application of the numerical approach as described before the developed routine was implemented into the pre- and postprocessor PEP (Programmers Environment for Pre-/Post-processing). The functionality of PEP provides an interface for the import of the (D)CTT diagrams in the form of tables as well as the visualization of the results for microstructures and hardness.

To validate the new numerical tool and to determine how sensitive the new developed routine predicts the microstructure experiments in laboratory as well as in the industrial scale were performed.

4.1. Laboratory Scale

The intention of the laboratory scale experiment was to verify the results for the $t_{8/5}$-time which are correlated with the (D)CTT-diagrams. In the experiment as shown in figure 8 a cylindrical specimen with a diameter of 20 mm and a height of 20 mm is heated up to 1250 °C and cooled at resting air down to room temperature. The material properties for the cooling simulation with the implicit FEM-solver Larstran/Shape were adopted from the HDB-steel.

Since the forging did not proceed in this experiment only the continuous cooling at resting air was considered in the FEM-simulation. The FEM-model of the specimen was reduced to a 2-dimensional model of a quarter of the cross section of the specimen due to its cylindrical shape. Without a forging step the initial values for the temperature (T_0 = 1250 °C) and the plastic strain ($\varepsilon_{v0} = 0$) are constant for the whole specimen. Figure 9 shows the result for the calculated $t_{8/5}$-time in this experiment.

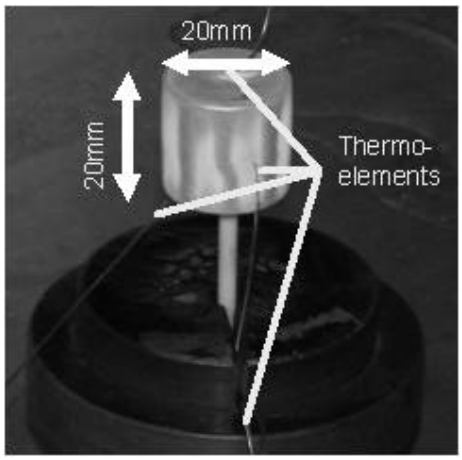

Fig. 8. *Experimental setup in laboratory scale.*

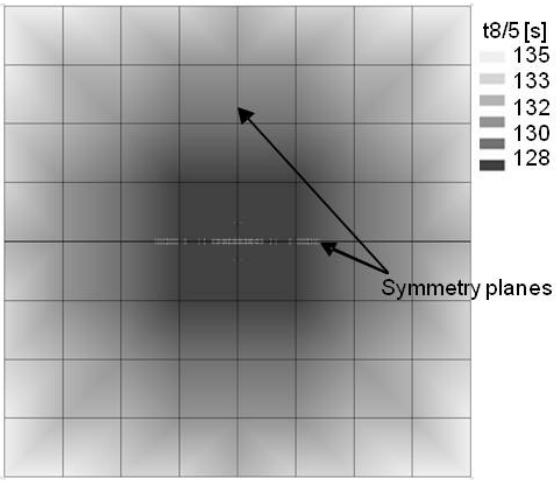

Fig. 9. *Calculated values for the $t_{8/5}$-time in the section view of the specimen.*

In a further step the hardness and the microstructure were identified for each node of the FE-mesh by correlating the $t_{8/5}$-time, the plastic strain and the temperature after forming in the part with the information of the (D)CTT diagram. The comparison of the hardness values extracted from the experiment and the new approach shows a good agreement in the results (see table 3).

Table 3. *Hardness of the specimen after cooling.*

	max{*HV10*}	**min{*HV10*}**
Simulation	433.1	433.0
Experiment	431	401

4.2. Industrial Scale

After the validation in laboratory scale the experiments were extended to industrial scale. The experiments were executed at Hirschvogel Umformtechnik GmbH and comprised in forging a common rail (see figure 10) of an injection system using the new developed HDB-steels Pilot 1 and Pilot 2. In the experiments a cylindrical specimen was heated up to 1250°C, next forged in a 3 steps closed die process to its final shape and cooled at resting air within the cooling zone. After reaching a temperature of approximately 450°C at the end of the cooling zone the forged parts were stored together in an open box.

Fig. 10. *Forged common rail (source: Hirschvogel Umformtechnik GmbH).*

The experimental scenario of forging and cooling the part was considered in the FEM-simulation as well. The required material properties were taken from the HDB-steel. The results of the forging simulation gained with Forge2008 were mapped to the simulation of the cooling at resting air with Larstran/Shape. The cooling of the forged parts in the box could not be simulated due to its undefined boundary conditions. To provide the expected microstructure and hardness the simulated temperature history, as well as the temperature and strain distribution after forging, was imported in PEP. The automatic calculation of $t_{8/5}$ and the correlation with the (D)CTT-diagram were applied. To verify the simulated results the microstructure results were compared at three different part sections and in addition the temperature history was compared at point D as illustrated in figure 11.

In the series of forging tests with the Pilot 1 alloy the temperature history at point D was measured by the use of a pyrometer to prove the simulated temperature results. Without any adaption of the model parameters the simulated and experimentally measured temperature history showed a good agreement (see figure 12).

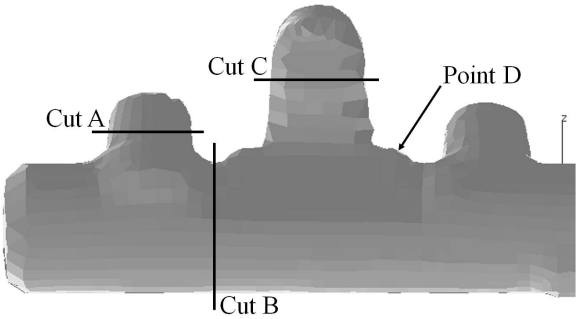

Fig. 11. *Sections in the spatial shape of the forged common rail*

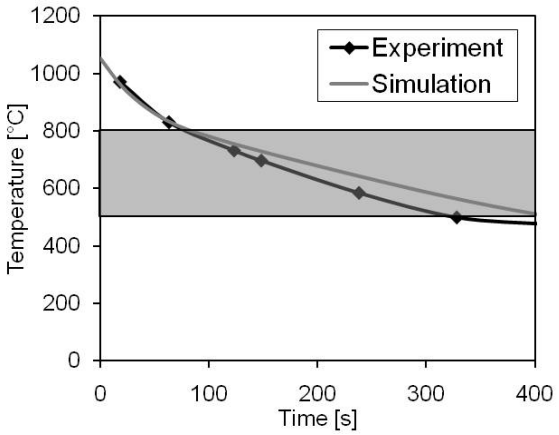

Fig. 12. *Simulated vs. experimentally measured temperature history at point D.*

In a further step comparisons were made between the predicted and the experimental measured microstructure for both the Pilot 1 and the Pilot 2 alloy. To provide the transformation properties (D)CTT diagrams were recorded for both alloys. Regarding the Pilot 2 alloy the utilized (D)CTT diagram is shown in figure 1. In case of the Pilot 1 alloy the predicted microstructure and hardness match the experimental results as shown in tables 4 and 5.

Table 4. *Bainite fraction [%] of the common rail after cooling (Pilot 1).*

	Simulation	Experiment
Cut A	96% – 97%	100%
Cut B	95% – 96%	97%
Cut C	95% – 96%	100%

Table 5. *HV10 of the common rail after cooling (Pilot 1).*

	Simulation	Experiment
Cut A	360 – 363	375 – 383
Cut B	369 – 383	375
Cut C	381 – 386	383 – 392

For the Pilot 2 alloy the predicted microstructure and hardness results show high deviations compared to the experimental results (see table 6 and table 7). Here, the discrepancies may have been caused by the conditions of the industrial process. As mentioned, in the industrial process the forged parts are collected in an open box at the end of the continuous cooling at resting air. Due to the limited length of the cooling zone the parts have a temperature of approximately 450 °C when they reach the end of the cooling section. The further cooling in the open box is hard to capture, in any case the cooling will be slower because of the concentrated heat of all stored parts. In case that the bainitic phase transformation is not finished during the continuous cooling at resting air, the decelerated cooling in the box will have a decisive effect on the resulting microstructure. Considering the transformation behavior described by the (D)CTT diagrams, the Pilot 2 alloy should consist of a partially bainitic and partially martensitic microstructure after the cooling at resting air, whereas the Pilot 1 alloy should reach an almost complete bainitic microstructure. Therefore, the differences between experiment and simulation in alloy Pilot 2 can be explained by the insufficient knowledge of the cooling process for the stored parts where the bainitic phase transformation is promoted and thereby extends the bainite phase fraction. An improvement can be achieved by adjusting the data base for the model to the requirements of the cooling process after forging and extending the controlled cooling process to temperatures below the end of the bainitic phase transformation.

Table 6. *Bainite fraction [%] of the common rail after cooling (Pilot 2).*

	Simulation	Experiment
Cut A	54% – 62%	99%
Cut B	65% – 75%	98%
Cut C	51% – 54%	98%

Table 7. *HV10 of the common rail after cooling (Pilot 2).*

	Simulation	Experiment
Cut A	460 – 461	392 – 401
Cut B	446 – 470	401 – 411
Cut C	480 – 481	421

Further enhancement of the predicted results may be reached by recording the (D)CTT diagrams with respect to the latent heat during phase transformation. The release of energy during phase trans-

formation leads to a temporary increase of the temperature and extends the cooling process. In the context of this project the (D)CTT diagrams were recorded in dilatometer tests using an exponential cooling function. More accuracy may be achieved by running the cooling in the dilatometer test with a modified cooling function which takes the latent heat into account.

5. CONCLUSIONS

The developed HDB-steel allows the production of forged components with high strength and good toughness without an additional heat treatment. A cooling strategy adjusted to the bainitic microstructure leads to a cost effective process chain of the high strength and ductile forged components.

To identify process parameters and to predict the microstructure and hardness distribution in the forged component, a numerical approach has been developed. In the applied approach, the results of forging and cooling simulations with commercial FEM solvers are correlated with the (D)CTT-diagrams to predict the microstructure and hardness distribution in forged parts. In the current state the method requires a continuous cooling down to low temperatures to obtain a sufficient accuracy. To provide an easy interpretation and visualization of these results the numerical approach was implemented into a pre- and postprocessor tool.

ACKNOWLEDGMENTS

The authors acknowledge the support of IMU (Industrieverband Massivumformung e. V.) and AiF (Arbeitsgemeinschaft industrieller Forschungsvereinigungen "Otto von Guericke" e.V.) for the project AiF 09390 06 ZN. The authors also would like to express their thanks to the industrial project partners CDP Bharat Forge GmbH, Deutsche Edelstahlwerke GmbH, Edelstahlzieherei Mark GmbH, Georgsmarienhütte GmbH, Hammerwerk Fridingen GmbH, Hirschvogel Umformtechnik GmbH, Johann Hay GmbH & Co. KG, Karl Diederichs KG, Saarstahl AG and ThyssenKrupp Gerlach GmbH.

REFERENCES

Bhadeshia, H.K.D.H., 2001, *Bainite in steels*, IOM Communications Ltd., 2nd Ed., Cambridge University Press, London.

Cristinacce, M., Reynolds, P. E., 1996, *Fundamentals and Applications of Microalloying Forging Steels*, TMS, Warrendale, PA, 29-43.

Fang, F., Yong, Q., Yang, C., Su, H., 2009, Microstructure and Precipitation Behavior in HAZ of V and Ti Microalloyed Steel, *Steel Research International*, 16, 68-72, 77.

Fischer, M., Gerdemann, F., Bleck, W., 2009, Object based quantitative analysis of complex multiphase microstructures in steel, *TMS 2009 – 138th Annual Meeting & Exhibition*, San Francisco (CA), 101-109.

Gladman, T., 1997, *The Physical Metallurgy of Microalloyed Steels*, The Institute of Materials, London, 341-348.

Johnson, A.W., Jacobson, S.H., 2002, On the convergence of generalized hill climbing algorithms, *Discrete Applied Mathematics*, 119 (1-2), 37-57.

Lemaitre, C., Dierickx, P., 2006, Steels for high performance diesel engines, *New Development in Long and Forged Products Proceedings*, 29-36.

NUMERYCZNE PRZEWIDYWANIE MIKROSTRUKTURY W WYSOKO WYTRZYMAŁYCH, PLASTYCZNYCH ODKUWKACH

Streszczenie

Przemysł samochodowy charakteryzuje ciągły wzrost zapotrzebowania na lżejsze, bardziej wytrzymałe i przy tym tańsze części, aby możliwe było utrzymanie ekonomicznego i technologicznego postępu. Połączenie wysokiej wytrzymałości i plastyczności jest wymagane szczególnie w przypadku części mających wpływ na bezpieczeństwo. Aby spełnić te wymagania, celem niniejszej pracy jest poprawa własności mechanicznych stali poprzez zastosowanie wysokowytrzymałych, plastycznych stali o strukturze bainitycznej, przy utrzymaniu efektywnego ekonomicznie procesu wytwarzania dla stali wysokowytrzymałych. W tym celu opracowano nowy skład chemiczny stali i zaproponowano cykl wytwarzania tej stali. Dla zmniejszenia liczby kosztownych badań doświadczalnych do identyfikacji parametrów procesu i kształtu przedkuwek, które umożliwiłyby uzyskanie docelowej mikrostruktury, opracowano numeryczny model przewidujący rozwój mikrostruktury stali w trakcie wytwarzania. Model numeryczny opiera się na symulacjach MES procesów kucia I chłodzenia połączonych z wykresami odkształcenie-chłodzenie-czas-temperatura-przemiana.

Received: July 28, 2010
Received in a revised form: September 17, 2010
Accepted: October 12, 2010